Microporous Materials

International Edition: DOI: 10.1002/anie.201509213
German Edition: DOI: 10.1002/ange.201509213

Zeolitic Imidazolate Framework/Graphene Oxide Hybrid Nanosheets as Seeds for the Growth of Ultrathin Molecular Sieving Membranes

*Yaoxin Hu, Jing Wei, Yan Liang, Huacheng Zhang, Xiwang Zhang, Wei Shen, and Huanting Wang**

Abstract: *A defect-free zeolitic imidazolate framework-8 (ZIF-8)/graphene oxide (GO) membrane with a thickness of 100 nm was prepared using two-dimensional (2D) ZIF-8/GO hybrid nanosheets as seeds. Hybrid nanosheets with a suitable amount of ZIF-8 nanocrystals were essential for producing a uniform seeding layer that facilitates fast crystal intergrowth during membrane formation. Moreover, the seeding layer acts as a barrier between two different synthesis solutions, and self-limits crystal growth and effectively eliminates defects during the contra-diffusion process. The resulting ultrathin membranes show excellent molecular sieving gas separation properties, such as with a high CO_2/N_2 selectivity of 7.0. This 2D nano-hybrid seeding strategy can be readily extended to the fabrication of other defect-free and ultrathin MOF or zeolite molecular sieving membranes for a wide range of separation applications.*

Metal–organic framework (MOF) films have been studied for a wide range of applications, such as sensors, low-k dielectrics, and separation membranes.[1] In particular, MOF membranes have shown great potential for energy-efficient gas separation.[2] For industrial applications, ultrathin and defect-free MOF membranes are required to achieve high gas flux and thus reduce process costs. As a thin MOF layer does not have enough mechanical strength as a self-supporting membrane, it needs to be produced on a mechanically strong, porous support.[3] Despite various fabrication methods being developed, the fabrication of ultrathin MOF membranes is extremely challenging owing to the difficulty in controlling heterogeneous nucleation and growth on porous substrates. Only until very recently, Yang and co-workers demonstrated successful synthesis of freestanding MOF nanosheets with a large lateral area and high crystallinity from a layered MOF, and used them as building blocks for the preparation of ultrathin gas separation membrane.[4] Owing to similar crystallization mechanisms between MOFs and zeolites, the main strategies for synthesizing zeolite membranes have been widely adopted to fabricate MOF membranes.[5] The Tsapatsis and Li groups recently made breakthroughs in the preparation of ultrathin zeolite membranes by secondary growth of two-dimensional (2D) seeds consisting of their exfoliated nanosheets or slice-shaped zeolites.[6] These exciting developments demonstrate significant advantages of using nanosheets over isotropic nanoparticles,[7] and offer an avenue to fabricate high-performance molecular sieving membranes from layered MOFs and zeolites. However, the synthesis of crystalline nanosheets from non-layered MOFs and zeolites remains a significant challenge. There is still an urgent need to develop an effective method for the fabrication of mechanically stable MOF lamellae to construct ultrathin molecular sieving membranes from a wide variety of other MOFs and zeolite materials.

Two-dimensional nanocomposites, such as graphene oxide (GO) nanosheets and MOFs/zeolites, have been the focus of recent research owing to their unique properties.[8] A number of their composites such as ZIF-67/GO,[9] silicalite/GO,[10] MOF-5/GO,[11] HKUST-1/GO,[12] MIL-100/GO,[13] MIL-53/GO,[14] and ZIF-8/GO[15] have been reported by our group and many others. Caro and co-workers[2g] showed the effectiveness of using GO to seal MOF crystal gaps to improve gas selectivity of MOF membranes. These studies demonstrate that it is feasible to prepare GO hybrid nanosheets from different MOFs and zeolites to build up ultrathin molecular sieving membranes.

Herein, we report a strategy to fabricate ultrathin and defect-free molecular sieving membranes by secondary growth of 2D hybrid MOF/GO seeding layer on various porous substrates. Specifically, the hybrid MOF nanosheets are formed by growing MOF nanocrystals on both sides of 2D GO nanosheets. These flexible, micro-sized hybrid nanosheets allow for seeding substrates with large-pores and rough surface, eliminating substrate modification required in the conventional synthesis using nanocrystal seeds. In principle, this strategy has great potential to be developed as a platform technique for the fabrication of ultrathin molecular sieving membranes from various crystalline porous materials.

Zeolitic imidazolate framework-8 (ZIF-8) was chosen as an example to demonstrate our 2D nano-hybrid seeding strategy. As one important subclass of MOFs, ZIFs exhibiting high thermal and chemical stability are very attractive for membrane applications.[1c–e] Although a great deal of work has been conducted in the fabrication of ZIF membranes, ultrathin ZIF membranes have not been reported so far. ZIF-8 ($Zn(mim)_2$, Hmim = 2-methylimidazolate) has sodalite structure and a pore window size of about 0.34 nm, which is just between the molecular sizes of CO_2 (0.33 nm) and N_2 (0.36 nm). Therefore, a defect-free ZIF-8 membrane is expected to achieve a good molecular sieving of CO_2 and N_2, which has important implications for many applications, such as CO_2 capture from flue gas. As illustrated in Figure 1,

[*] Y. X. Hu, Dr. J. Wei, Y. Liang, Dr. H. C. Zhang, Prof. X. W. Zhang, Prof. W. Shen, Prof. H. T. Wang
Department of Chemical Engineering, Monash University
Clayton, Victoria 3800 (Australia)
E-mail: huanting.wang@monash.edu

Supporting information for this article is available on the WWW under http://dx.doi.org/10.1002/anie.201509213.

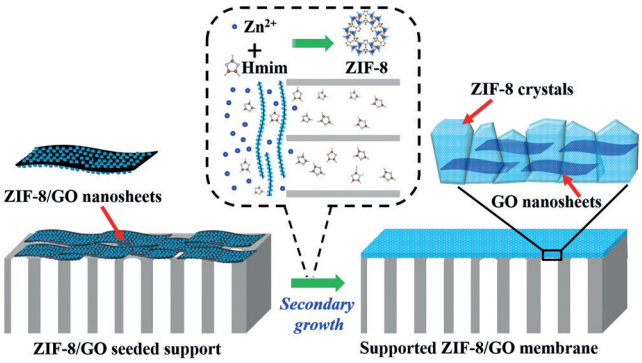

Figure 1. Illustration of the synthesis process of ultrathin ZIF-8/GO membrane: coating of flexible ZIF-8/GO nanosheets on a porous support, such as anodic aluminium oxide (AAO), and subsequent secondary growth by the contra-diffusion method.

an ultrathin ZIF-8 membrane supported on a porous support, such as an anodic aluminium oxide (AAO) disc, was fabricated using ZIF-8/GO nanosheets as seeding and subsequent secondary growth. 2D ZIF-8/GO hybrid seeds were prepared by adding GO solution into the precursors including the metal ion (Zn^{2+}) and the organic ligand (Hmim) at room temperature. ZIF-8 nanoparticles grew on both sides of the GO nanosheets surface to obtain ZIF-8/GO/ZIF-8 nanosheets with a sandwich-like structure. The seeding layer composed of laminated nanosheets was prepared by spin-coating of a ZIF-8/GO methanol suspension on the porous AAO twice for complete and uniform surface coverage. Finally, the ZIF-8/GO membrane was synthesized by secondary growth using the contra-diffusion method (also known as the interfacial synthesis).[2f,16] The seeding layer constructed by 2D hybrid nanosheets provide 2D confined space and uniform coating of ZIF-8 nanocrystals to facilitate fast crystal intergrowth. Moreover, the seeding layer acts as a barrier between two different synthesis solutions, and effectively avoid crystal over-growth and defects during the contra diffusion process, leading to a defect-free and ultrathin membrane.

Hybrid ZIF-8/GO nanosheets with different ZIF-8 loadings were synthesized by varying different synthesis time (20 min, 3 h, and 5 h), and denoted as seeds-20min, seeds-3h, and seeds-5h, respectively (Supporting Information, Figure S1a). X-ray diffraction (XRD) patterns showed that all as-synthesized nanosheets have pure ZIF-8 phase (Figure S2). The resulting 2D ZIF-8/GO hybrid nanosheets were also characterized by scanning electron microscopy (SEM) and transmission electron microscopy (TEM). For a short synthesis time (20 min), there was a low coverage of ultra-small ZIF-8 crystals on the GO nanosheets (Figure S1b,c and S3a). Seeds-20 min showed high flexibility (Figure S3b) and easily aggregated, leading to an uneven coverage of the support after spin coating (Figure 2a). For longer synthesis times (3 h or 5 h), the GO surface was fully covered by ZIF-8 nanoparticles (Figure S1d,e and S3c,e). The selected area electron diffraction (SAED) pattern of the seeds-3h (Figure S4) indicated ZIF-8 nanoparticles uniformly deposited on the GO surfaces were polycrystalline. Note that the micro-sized

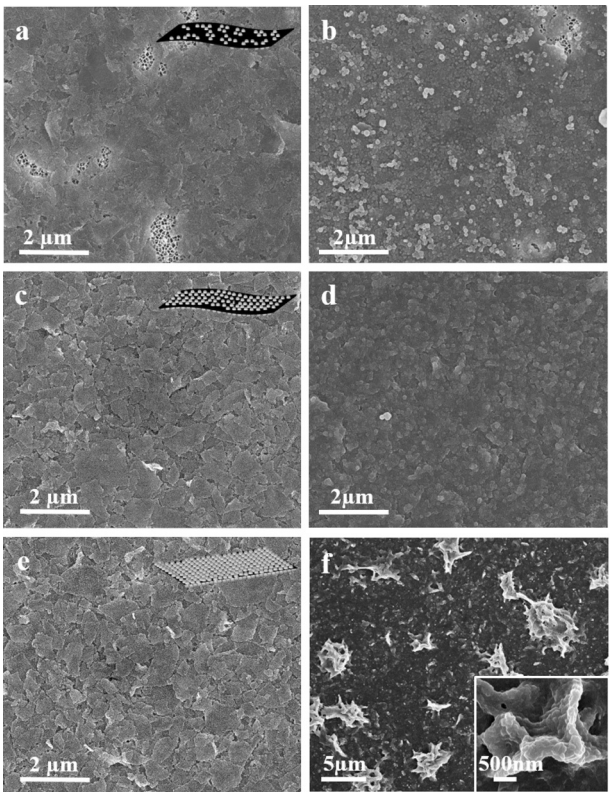

Figure 2. SEM images of the surface of seeding layer (a, c, e) and ZIF-8/GO membrane (b, d, f) after 1 h secondary growth from the seeding layer using (a, b) seeds-20min, (c, d) seeds-3h, and (e, f) seeds-5h. The inserts in a, c, and e are corresponding diagrams of hybrid ZIF-8/GO structure viewed from seeds-20min, seeds-3h, and seeds-5h. The insert in f is a high-magnification surface view.

ZIF-8/GO nanosheets were easily purified by washing away ZIF-8 nanoparticles grown in the synthesis solution (Figure S5). The sandwich-like seeds-3h and seeds-5h nanosheets resulted in evenly covered surface of the porous support after spin-coating (Figure 2c,e).

To investigate the effect of ZIF-8 loading of 2D hybrid seeds on membrane growth, seeded AAO supports with seeds-20min, seeds-3h and seeds-5h (Figure 2a,c,e) were used to synthesize ZIF-8/GO membranes by contra-diffusion secondary growth for 1 h. ZIF-8/GO membranes prepared using seeds-20min, seeds-3h or seeds-5h after 1 h secondary growth were denoted M-20m-1h, M-3h-1h, and M-5h-1h, respectively (Figure 2b,d,f). There were clearly defects on M-20min-1h owing to incomplete coverage of hybrid nanosheets on the support. While the uniform seeding layer was obtained from seeds-3h or seeds-5h, M-3h-1h was well inter-grown, showing flat and smooth surface. Some crossly grown hybrid flakes were observed in M-5h-1h, forming defects on the surface (Figure 2f). This is probably because seeds-5h nanosheets with a higher loading ZIF-8 nanocrystals are more rigid and less adaptive to the shape change occurring in the contra-diffusion secondary growth process, and the higher loading of ZIF-8 in seeds-5h results in faster secondary growth, pushing some nanosheets upward. By contrast, seeds-3h has a balanced flexibility and ZIF-8 loading. The flexibility of seeds-3h

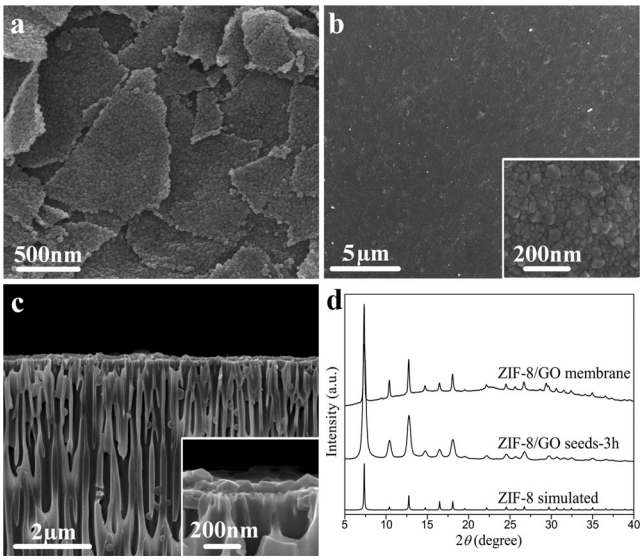

Figure 3. SEM images of the seeds-3h powder (a), and the surface (b) and cross-section (c) of ZIF-8/GO membrane (M-3h-3h) on the AAO substrate. d) XRD patterns of simulated ZIF-8 structure, seeds-3h and ZIF-8/GO membrane (M-3h-3h). The inset in b is a high-magnification surface view, and c is a high-magnification cross-sectional view.

was confirmed by SEM. As shown in Figure 3a, seeds-3h can be bent by fast solvent evaporation in the SEM specimen preparation. Flexible seeds-3h is beneficial for achieving a conformal layer on porous support even with a rough surface. The AAO surface was uniformly covered by the hybrid nanosheets, and the seeding layer thickness is about 100 nm (Figure S3d and S6). The thermogravimetric analysis (TGA) result (Figure S7) showed that the hybrid ZIF-8/GO nanosheets (seeds-3h) have excellent thermal stability, indicating the ZIF-8 is well crystallized; the actual content of GO in hybrid ZIF-8/GO nanosheets is calculated to be 2.3 wt%. Comparison of these different seeds showed that the ZIF-8 loading of hybrid nanosheets was crucial for uniform seeding of porous support and successful growth of ultrathin membrane during secondary growth.

For comparison, when ZIF-8 nanoparticles and GO suspension were simply mixed, ZIF-8 nanocrystals and GO nanosheets severely aggregated, and no uniform seeding layer on the AAO support was obtained (Figure S8). Without ZIF-8/GO hybrid seeds, a non-continuous ZIF-8 layer was produced on the Zn^{2+} solution side, whereas a thick and fragile ZIF-8 layer was formed on the Hmim side (Figure S9). Our further gas separation experiments confirmed that the seeds-3h exhibited balanced amount of ZIF-8 nanocrystals covered on GO and flexibility to form high-quality membranes. We also found that when the secondary growth time was extended to 3 h, the resulting membrane (denoted M-3h-3h) had better gas permeation selectivity (shown below). Therefore, M-3h-3h was chosen for further studies.

The ZIF-8/GO layer (M-3h-3h) was composed of well-intergrown ZIF nano-grains, and had a thickness of about 100 nm (Figure 3b,c), which is about 4–200 times thinner than reported ZIF-8 membranes.[1c,2e–g,17] Cross-sectional SEM images also revealed that only some scattered ZIF-8 nanocrystals are formed inside the AAO porous channels (Figure 3c). This is because the seeding layer functions as an effective barrier between two synthesis precursor solutions, leading to crystal growth around the hybrid nanosheets, and thus limiting diffusion of Zn^{2+} ions into the porous channels. In contrast, the membrane synthesis without seeds results in a poorly intergrown film, with ZIF-8 crystals observed on both sides and inside porous channels of the AAO support (Figure S9). This further demonstrates that the hybrid nanosheets play a key role in the growth of ultrathin, defect-free ZIF-8 membranes. XRD patterns (Figure 3d) show that both M-3h-3h membrane and seeding have a high degree of crystallinity, and all of the peaks match well with those of the simulated ZIF-8 structure.[18]

The single-gas permeation properties of the ZIF-8/GO membranes fabricated using the hybrid nanosheets as seeds were investigated for H_2, CO_2, N_2, CH_4, C_3H_6, and C_3H_8 gases by the constant-volume/variable-pressure method.[16b,17e] Table S1 shows the H_2 and N_2 gas permeation results of four different membranes (M-20m-1h, M-3h-1h, M-5h-1h, and M-3h-3h). After 1 h secondary growth, the membrane (M-3h-1h) has a H_2 gas permeance of 9.5×10^{-8} mol m^{-2} s^{-1} pa^{-1} and the highest H_2/N_2 selectivity of 8.9 compared with M-20m-1h and M-5h-1h. Further increasing the secondary growth time leads to an increase in gas selectivity. M-3h-3h exhibits a higher H_2/N_2 selectivity (11.1) owing to reduced non-selective defects from longer secondary growth. Figure 4 shows the single gas

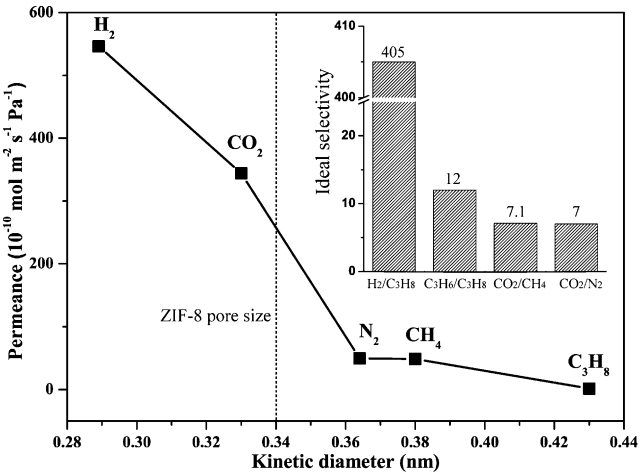

Figure 4. Single gas permeances of different gases through ZIF-8/GO membrane (M-3h-3h) at 25 °C and 1 bar as a function of the kinetic diameter. The inset shows the ideal gas selectivity for H_2/C_3H_8, C_3H_6/C_3H_8, CO_2/CH_4, and CO_2/N_2. ZIF-8 pore size (dashed line) estimated from crystal structure data.[18]

permeance of the ZIF-8/GO membrane (M-3h-3h) as a function of the kinetic diameter of the gas molecule at 25 °C and 1 bar. The H_2 permeance is 5.46×10^{-8} mol m^{-2} s^{-1} pa^{-1}, which is much greater compared with other gases (Table S2). The permeance clearly depends on the gas molecular size. There is a clear cut-off between CO_2 and N_2 with a selectivity of 7.0, which is the highest CO_2/N_2 selectivity among the best ZIF-8 membranes reported (Table S3). This is strong evidence that

the ZIF-8/GO membrane is of high-quality. Owing to the well-known framework flexibility, the molecules with a kinetic diameter larger than the crystallographic pore size of ZIF-8 (0.34 nm), such as N_2, CH_4, C_3H_6, and C_3H_8 can also pass through the ZIF-8 membrane.[1c,19] As shown in Table S2, the ideal selectivity measured at 25 °C and 1 bar is 11.1 and 405.0 for H_2/N_2 and H_2/C_3H_8, respectively, which by far exceed their corresponding Knudsen selectivity (3.7 and 4.7); The H_2/N_2 selectivity surpasses the reported H_2/N_2 ideal selectivity (4.67) of ZIF-8/AAO membrane.[20] Furthermore, our membrane also shows high propylene/propane separation property with an ideal selectivity of 12 at 25 °C, which is comparable with reported ZIF-8 membranes.[2e,f,17c] M-3h-3h membrane also exhibits a good CO_2 permeance (3.44×10^{-8} mol m^{-2} s^{-1} pa^{-1}) and a high ideal CO_2/CH_4 selectivity (7.1). As shown in Table S3, the ultrathin ZIF-8/GO membrane prepared in this work has excellent molecular sieving properties, which are among the best reported (Table S3).

To demonstrate the versatility of our new seeding method, we have successful prepared ZIF-8/GO membrane on a porous polymer support. In particular, a porous Nylon membrane with rough surface was chosen as the substrate (STERLITECH, 80 μm thick and 100 nm pore size, Figure S10a). A similar procedure for the preparation of ZIF-8/GO membrane on the AAO support was used, and a dense ZIF-8/GO top layer was formed on the one side of the Nylon substrate within 3 h (Figure S10). The XRD pattern of the ZIF-8/GO membrane on the Nylon support exhibits characteristic peaks of a pure ZIF-8 crystal structure (Figure S11). The membrane formation is much faster than the growth of ZIF-8 membranes on Nylon substrate through the same contra-diffusion method,[16b,21] the latter required at least 16 h synthesis.

It is worth noting that GO used in the preparation of 2D seeds are impermeable to gases,[22] and this would increase gas permeation resistance. Several techniques have been reported to create nanoporous GO,[23] and therefore it is highly feasible to prepare nanoporous ZIF/GO nanosheets for the fabrication of ultrathin molecular sieving membranes with improved gas permeability. Furthermore, the resultant membranes show better mechanical stability than those prepared without using ZIF/GO nanosheets (Figure S9a and S12).

In conclusion, we have developed a simple and versatile 2D nano-hybrid seeding strategy for the preparation of ultrathin, defect-free ZIF membranes. The ZIF-8/GO membrane, with a thickness of about 100 nm, was prepared using 2D ZIF-8/GO nanosheets as seeds and subsequent 3 h secondary growth. The thickness of ZIF-8/GO membranes is one of the thinnest ever reported, and its separation performance is among the best ZIF-8 membranes reported so far. At 25 °C and 1 bar, the ZIF-8/GO membrane has an ideal separation selectivity of 405 for H_2/C_3H_8 and 7 for CO_2/N_2. Furthermore, ZIF-8/GO membranes were also successfully fabricated on the porous Nylon substrate using the hybrid nanosheets as seeds. We anticipate that the concept of using 2D nano-hybrid seeding may be further developed to grow defect-free and ultrathin MOFs or zeolites molecular sieve membranes with other crystal structures for different separation applications.

Acknowledgements

This work was supported by the Australian Research Council through a Future Fellowship project (Huanting Wang, FT100100192). The authors thank the staff of Monash Centre for Electron Microscopy at Monash University for their technical assistance with SEM and TEM.

Keywords: gas separation · graphene oxide · membranes · metal–organic frameworks · zeolitic–imidazolate frameworks

How to cite: *Angew. Chem. Int. Ed.* **2016**, *55*, 2048–2052
Angew. Chem. **2016**, *128*, 2088–2092

[1] a) H. Furukawa, K. E. Cordova, M. O'Keeffe, O. M. Yaghi, *Science* **2013**, *341*, 6149; b) S. Qiu, M. Xue, G. Zhu, *Chem. Soc. Rev.* **2014**, *43*, 6116–6140; c) J. Yao, H. Wang, *Chem. Soc. Rev.* **2014**, *43*, 4470–4493; d) H. Hayashi, A. P. Côté, H. Furukawa, M. O'Keeffe, O. M. Yaghi, *Nat. Mater.* **2007**, *6*, 501–506; e) Y. Lin, *Curr. Opin. Chem. Eng.* **2015**, *8*, 21–28.

[2] a) H. Bux, F. Liang, Y. Li, J. Cravillon, M. Wiebcke, J. Caro, *J. Am. Chem. Soc.* **2009**, *131*, 16000–16001; b) S. R. Venna, M. A. Carreon, *J. Am. Chem. Soc.* **2010**, *132*, 76–78; c) A. Huang, J. Caro, *Angew. Chem. Int. Ed.* **2011**, *50*, 4979–4982; *Angew. Chem.* **2011**, *123*, 5083–5086; d) A. W. Thornton, D. Dubbeldam, M. S. Liu, B. P. Ladewig, A. J. Hill, M. R. Hill, *Energy Environ. Sci.* **2012**, *5*, 7637–7646; e) Q. Liu, N. Wang, J. Caro, A. Huang, *J. Am. Chem. Soc.* **2013**, *135*, 17679–17682; f) A. J. Brown, N. A. Brunelli, K. Eum, F. Rashidi, J. R. Johnson, W. J. Koros, C. W. Jones, S. Nair, *Science* **2014**, *345*, 72–75; g) A. Huang, Q. Liu, N. Wang, Y. Zhu, J. Caro, *J. Am. Chem. Soc.* **2014**, *136*, 14686–14689; h) Y. Liu, N. Wang, J. H. Pan, F. Steinbach, J. Caro, *J. Am. Chem. Soc.* **2014**, *136*, 14353–14356; i) Y. Pan, W. Liu, Y. Zhao, C. Wang, Z. Lai, *J Memb Sci.* **2015**, *493*, 88–96; j) D. Liu, X. Ma, H. Xi, Y. S. Lin, *J. Membr. Sci.* **2014**, *451*, 85–93.

[3] J. Caro, *Chem. Soc. Rev.* **2016**, DOI: 10.1039/c5s00597c.

[4] Y. Peng, Y. Li, Y. Ban, H. Jin, W. Jiao, X. Liu, W. Yang, *Science* **2014**, *346*, 1356–1359.

[5] a) N. Rangnekar, N. Mittal, B. Elyassi, J. Caro, M. Tsapatsis, *Chem. Soc. Rev.* **2015**, *44*, 7128–7154 ; b) Y. Hu, X. Dong, J. Nan, W. Jin, X. Ren, N. Xu, Y. M. Lee, *Chem. Commun.* **2011**, *47*, 737–739.

[6] a) K. V. Agrawal, B. Topuz, T. C. T. Pham, T. H. Nguyen, N. Sauer, N. Rangnekar, H. Zhang, K. Narasimharao, S. N. Basahel, L. F. Francis, C. W. Macosko, S. Al-Thabaiti, M. Tsapatsis, K. B. Yoon, *Adv. Mater.* **2015**, *27*, 3243–3249; b) Y. Huang, L. Wang, Z. Song, S. Li, M. Yu, *Angew. Chem. Int. Ed.* **2015**, *54*, 10843–10847; *Angew. Chem.* **2015**, *127*, 10993–10997; c) K. Varoon, X. Zhang, B. Elyassi, D. D. Brewer, M. Gettel, S. Kumar, J. A. Lee, S. Maheshwari, A. Mittal, C. Y. Sung, M. Cococcioni, L. F. Francis, A. V. McCormick, K. A. Mkhoyan, M. Tsapatsis, *Science* **2011**, *334*, 72–75; d) M. Tsapatsis, *Science* **2011**, *334*, 767–768.

[7] T. Rodenas, I. Luz, G. Prieto, B. Seoane, H. Miro, A. Corma, F. Kapteijn, F. X. Llabrés I Xamena, J. Gascon, *Nat. Mater.* **2015**, *14*, 48–55.

[8] a) Q. L. Zhu, Q. Xu, *Chem. Soc. Rev.* **2014**, *43*, 5468–5512; b) J. W. Suk, R. D. Piner, J. An, R. S. Ruoff, *ACS Nano* **2010**, *4*, 6557–6564.

[9] J. Wei, Y. Hu, Z. Wu, Y. Liang, S. Leong, B. Kong, X. Zhang, D. Zhao, G. P. Simon, H. Wang, *J. Mater. Chem. A* **2015**, *3*, 16867–16873.

[10] D. Li, L. Qiu, K. Wang, Y. Zeng, D. Li, T. Williams, Y. Huang, M. Tsapatsis, H. T. Wang, *Chem. Commun.* **2012**, *48*, 2249–2251.

[11] a) C. Petit, T. J. Bandosz, *Adv. Mater.* **2009**, *21*, 4753 – 4757; b) M. Jahan, Q. Bao, J. X. Yang, K. P. Loh, *J. Am. Chem. Soc.* **2010**, *132*, 14487 – 14495.
[12] C. Petit, J. Burress, T. J. Bandosz, *Carbon* **2011**, *49*, 563 – 572.
[13] C. Petit, T. J. Bandosz, *Adv. Funct. Mater.* **2011**, *21*, 2108 – 2117.
[14] Y. Zhang, G. Li, H. Lu, Q. Lv, Z. Sun, *RSC Adv.* **2014**, *4*, 7594 – 7600.
[15] a) R. Kumar, K. Jayaramulu, T. K. Maji, C. N. R. Rao, *Chem. Commun.* **2013**, *49*, 4947 – 4949; b) X. Qiu, X. Wang, Y. Li, *Chem. Commun.* **2015**, *51*, 3874 – 3877; c) X. Huang, B. Zheng, Z. Liu, C. Tan, J. Liu, B. Chen, H. Li, J. Chen, X. Zhang, Z. Fan, W. Zhang, Z. Guo, F. Huo, Y. Yang, L. H. Xie, W. Huang, H. Zhang, *ACS Nano* **2014**, *8*, 8695 – 8701; d) X. Cao, B. Zheng, X. Rui, W. Shi, Q. Yan, H. Zhang, *Angew. Chem. Int. Ed.* **2014**, *53*, 1404 – 1409; *Angew. Chem.* **2014**, *126*, 1428 – 1433; e) H. X. Zhong, J. Wang, Y. W. Zhang, W. L. Xu, W. Xing, D. Xu, Y. F. Zhang, X. B. Zhang, *Angew. Chem. Int. Ed.* **2014**, *53*, 14235 – 14239; *Angew. Chem.* **2014**, *126*, 14459 – 14463; f) J. Wei, Y. Hu, Y. Liang, B. Kong, J. Zhang, J. Song, Q. Bao, G. P. Simon, S. P. Jiang, H. Wang, *Adv. Funct. Mater.* **2015**, *25*, 5768 – 5777.
[16] a) R. Ameloot, F. Vermoortele, W. Vanhove, M. B. J. Roeffaers, B. F. Sels, D. E. De Vos, *Nat. Chem.* **2011**, *3*, 382 – 387; b) J. Yao, D. Dong, D. Li, L. He, G. Xu, H. Wang, *Chem. Commun.* **2011**, *47*, 2559 – 2561.
[17] a) Y. Pan, B. Wang, Z. Lai, *J Memb Sci.* **2012**, *421 – 422*, 292 – 298; b) J. Yang, Z. Xie, H. Yin, J. Wang, J. Xu, J. Wang, J. Lu, D. Yin, Y. Zhang, *Microporous Mesoporous Mater.* **2014**, *198*, 263 – 270; c) Y. Pan, Z. Lai, *Chem. Commun.* **2011**, *47*, 10275 – 10277; d) H. Bux, A. Feldhoff, J. Cravillon, M. Wiebcke, Y. S. Li, J. Caro, *Chem. Mater.* **2011**, *23*, 2262 – 2269; e) O. Shekhah, R. Swaidan, Y. Belmabkhout, M. Du Plessis, T. Jacobs, L. J. Barbour, I. Pinnau, M. Eddaoudi, *Chem. Commun.* **2014**, *50*, 2089 – 2092; f) B. R. Pimentel, A. Parulkar, E. K. Zhou, N. A. Brunelli, R. P. Lively, *ChemSusChem* **2014**, *7*, 3202 – 3240; g) V. M. Aceituno Melgar, J. Kim, M. R. Othman, *J. Ind. Eng. Chem.* **2015**, *28*, 1 – 15.
[18] K. S. Park, Z. Ni, A. P. Côté, J. Y. Choi, R. Huang, F. J. Uribe-Romo, H. K. Chae, M. O'Keeffe, O. M. Yaghi, *Proc. Natl. Acad. Sci. USA* **2006**, *103*, 10186 – 10191.
[19] B. Chen, Z. Yang, Y. Zhu, Y. Xia, *J. Mater. Chem. A* **2014**, *2*, 16811 – 16831.
[20] M. He, J. Yao, Z. X. Low, D. Yu, Y. Feng, H. Wang, *RSC Adv.* **2014**, *4*, 7634 – 7639.
[21] M. He, J. Yao, L. Li, Z. Zhong, F. Chen, H. Wang, *Microporous Mesoporous Mater.* **2013**, *179*, 10 – 16.
[22] a) R. R. Nair, H. A. Wu, P. N. Jayaram, I. V. Grigorieva, A. K. Geim, *Science* **2012**, *335*, 442 – 444; b) H. Li, Z. Song, X. Zhang, Y. Huang, S. Li, Y. Mao, H. J. Ploehn, Y. Bao, M. Yu, *Science* **2013**, *342*, 95 – 98.
[23] a) Y. Lin, X. Han, C. J. Campbell, J. W. Kim, B. Zhao, W. Luo, J. Dai, L. Hu, J. W. Connell, *Adv. Funct. Mater.* **2015**, *25*, 2920 – 2927; b) Y. Xu, C. Y. Chen, Z. Zhao, Z. Lin, C. Lee, X. Xu, C. Wang, Y. Huang, M. I. Shakir, X. Duan, *Nano Lett.* **2015**, *15*, 4605 – 4610.

Received: October 1, 2015
Revised: November 4, 2015
Published online: December 28, 2015

